

### **Point-to-point responses to the comments:**

The authors addressed most of my concerns. However, I think there are still a few small issues:

*Response:* Many thanks to the reviewer for the comments and suggestions. Here I describe the point-to-point responses to the comments and questions.

1. Verb tense consistency in the paper is still sometimes an issue.

*Response:* The past tense is used in the descriptions for the experiments, and the present tense is used in the general narration. We have carefully checked and revised the full text again.

2. More importantly, though, I am still a bit confused by the statements about the PM emissions being higher for hot start state with respect to cold start state, that's a bit counterintuitive for me. It would be good to comment on some possible explanations for these statements/findings. For example, at line 471 the authors mention: "The PM emission was the highest under the hot stabilized running state, followed by those under the hot start, cold start" (this is mentioned also in other parts of the paper) but looking at figures 3 and 4, it seems to me that during the cold start state the vehicle emitted substantially more particles than during the hot start state. Am I misinterpreting the sentences, or am I misreading the figures, or is there a contradiction? Anyway, it would be good to clarify this and to provide a potential explanation.

*Response:* Many thanks for pointing out the misleading description. Our results showed that the total PM emissions under hot start state were slightly higher than that of under the cold start state. The higher emissions under hot start state may be ascribed to the conducting time of the vehicle engine. The hot start test was conducted within 5 mins after the cold start test. PM emissions from GDI vehicles are relatively less affected by ambient temperature for engines warmed up for 30 min (Cotte et al., 2001). Therefore, the emissions under the hot start could be higher than, actually close to, that under the cold start state.

The particles shown in Figures 3 and 4 were only those in the size range of accumulation mode. Although the total PM emission were higher under hot start state than that under the cold start state, the comparison of particles in the size range of accumulation mode indicated that the emissions for particles in this size mode were higher under the cold start state than under the hot start state (Figures 3, 4). Under the cold start state, larger proportions of particles were present in the size range of accumulation mode particles. This can be attributed to the less efficiency of the vaporization of fuel droplets in the combustion cylinder under the cold start state (Chen et al., 2017).

In the revision, we added some explanations for these statements/findings in lines 296-308: “The higher emission of particle in term of number for the GDI vehicle under the hot start state can be ascribed to the experimental time of the vehicle engine. The hot start test in this study was conducted within 5 mins after the cold start test. The PM emissions from GDI vehicles were relatively less affected by ambient temperature for the initial 30 minutes during the warming up of the engines (Cotte et al., 2001). This may lead to the high value of the PM emission for the hot start state which is slightly higher than that for the cold start state. Although the total PM emission were higher under hot start state than that under the cold start state, the comparison of those in the size range of accumulation mode indicates that the particulate emissions for this mode of particles were higher under the cold start state than under the hot start state (Fig. 3). This can be attributed to the less efficiency of the vaporization of fuel droplets in the combustion cylinder under the cold start state (Chen et al., 2017).”

#### References:

- Cotte, H., Bessagnet, B., Blondeau, C., Mallet-Hubert, P.Y., Momique, J.C., Walter, C., Boulanger, L., Deleger, D., Jouvenot, G., Pain, C., and Rouveiolles, P.: Cold-start emissions from petrol and diesel vehicles according to the emissions regulations (from Euro 92 to Euro 2000), *Int J Vehicle Des*, 27, 275-285, 10.1504/IJVD.2001.001971, 2001.
- Chen, L., Liang, Z., Zhang, X., and Shuai, S.: Characterizing particulate matter emissions from GDI and PFI vehicles under transient and cold start conditions, *Fuel*, 189, 131-140, <http://doi.org/10.1016/j.fuel.2016.10.055>, 2017.

3. One of my previous comment was regarding the limitation of the study and the generality of the conclusions having the data being collected from only one vehicle. The authors partially addressed this in their response but did not make any change in the paper that really addresses this issue (if not just mentioning that doing TEM is time-consuming, that is an explanation of why they did what they did, but it does not address the fact that is still a limitation of the study). I think it would be beneficial and honest to clearly point out this caveat in the paper, specifically in the abstract and in the conclusions.

**Response:** We fully agree with the comments on the limitation of the present results.

To make this further clearer, in the revision, we added descriptions on this limitation in several places including the abstract and conclusion: we have added “a commercial GDI-engine gasoline vehicle” in line 39, line 489, line 492, line 494 and line 499.

We also mentioned this limitation in lines 241-246: “There are differences in emissions from vehicles to vehicles, even for vehicles with same model engines. Only one GDI vehicle, the type of which constitutes the majority of light-duty vehicles in China, was tested in this study. The representativeness of the present results remains unevaluated carefully with, such as, comparisons between vehicles to achieve broader statistical results, although the tests in the present studies were conducted under strict control conditions.”

4. A final technical question: At line 393 the authors mention: "... transformation of primary particles emitted by the GDI-engine vehicles could occur within 3.5 hours", however, earlier they mentioned that the equivalent aging time they subjected their particles to in the chamber was ~10 days (line 205), so how do the authors reconcile these two statements? Please clarify.

**Response:** The “3.5 hours” is for the chamber experiment and the “~10 days” is for the ambient atmospheric conditions. In the chamber, the aging or transformation of primary particles emitted by the GDI-engine vehicles could occur within 3.5 hours. The aging

experiments for the gasoline exhausts were carried out with a relatively high OH exposure compared to ambient conditions. The OH exposure at the end of the experiments reproduced extreme oxidation processes, which were equivalent to cases of an oxidation more than 10 days in ambient air.

In order to clarify this meaning, in lines 202-208, we rephrased the sentence “Assuming the 24 hr mean concentration of  $10^6$  OH molecules  $\text{cm}^{-3}$  in Beijing (Lu et al., 2013), the OH exposure at the end of the experiments reproduced extreme oxidation processes in the atmosphere, which is equivalent to cases of an oxidation more than 10 days.” into “The OH exposure at the end of the experiments reproduced extreme oxidation processes, which were equivalent to cases of an oxidation more than 10 days in Beijing ambient air if the 24-hour-mean concentration of OH is  $10^6$  molecules  $\text{cm}^{-3}$  (Lu et al., 2013).”

### **A list of all relevant changes made in the manuscript :**

1. Line 28, 44, 56-60, 196, 230, 239-240, 276-278, 283, 365, 376, 447, 456-464 and 469-471: We revised the verb tense.
2. Line 39: We added "... a commercial GDI-engine gasoline vehicle..."
3. Line 202-207: We rephrased "Assuming the 24 hr mean concentration of  $10^6$  OH molecules  $\text{cm}^{-3}$  in Beijing (Lu et al., 2013), the OH exposure at the end of the experiments reproduced extreme oxidation processes in the atmosphere, which is equivalent to cases of an oxidation more than 10 days." as "The OH exposure at the end of the experiments reproduced extreme oxidation processes, which were equivalent to cases of an oxidation more than 10 days in Beijing ambient air if the 24-hour-mean concentration of OH is  $10^6$  molecules  $\text{cm}^{-3}$  (Lu et al., 2013)."
4. Line 296-308: we added "The higher emission of particle in term of number for the GDI vehicle under the hot start state can be ascribed to the experimental time of the vehicle engine. The hot start test in this study was conducted within 5 mins after the cold start test. The PM emissions from GDI vehicles were relatively less affected by ambient temperature for the initial 30 minutes during the warming up of the engines (Cotte et al., 2001). This may lead to the high value of the PM emission for the hot start state which is slightly higher than that for the cold start state. Although the total PM emission were higher under hot start state than that under the cold start state, the comparison of those in the size range of accumulation mode indicates that the particulate emissions for this mode of particles were higher under the cold start state than under the hot start sate (Fig. 3). This can be attributed to the less efficiency of the vaporization of fuel droplets in the combustion cylinder under the cold start state (Chen et al., 2017)."
5. Line 39, line 489, line 492, line 494 and line 499: we added "a commercial GDI-engine gasoline vehicle".
6. Line 571: We added a reference "Cotte, H., Bessagnet, B., Blondeau, C., Mallet-Hubert, P.Y., Momique, J.C., Walter, C., Boulanger, L., Deleger, D., Jouvenot, G., Pain, C., and Rouveirrolles, P.: Cold-start emissions from petrol and diesel vehicles according to the emissions regulations (from Euro 92 to Euro 2000), *Int J Vehicle Des*, 27, 275-285, 10.1504/IJVD.2001.001971, 2001."

1 **Morphology and size of the particles emitted from a gasoline**  
2 **direct injection-engine vehicle and their ageing in an**  
3 **environmental chamber**

4  
5 Jiaoping Xing<sup>a,b</sup>, Longyi Shao<sup>a\*</sup>, Wenbin Zhang<sup>c</sup>, Jianfei Peng<sup>d</sup>, Wenhua wang<sup>a</sup>, Shijin  
6 Shuai<sup>c</sup>, Min Hu<sup>d</sup>, Daizhou Zhang<sup>c\*</sup>  
7

8 <sup>a</sup>State Key Laboratory of Coal Resources and Safe Mining, School of Geoscience and Survey  
9 Engineering, China University of Mining and Technology (Beijing), Beijing 100083, China.

10 <sup>b</sup>2011 Collaborative Innovation Center of Jiangxi Typical Trees Cultivation and Utilization, School of  
11 Forestry, Jiangxi Agricultural University, Nanchang, 330045, China.

12 <sup>c</sup>State Key Laboratory of Automotive Safety and Energy, Department of Automotive Engineering,  
13 Tsinghua University, Beijing 100084, China

14 <sup>d</sup>State Key Joint Laboratory of Environmental Simulation and Pollution Control, College of  
15 Environmental Sciences and Engineering, Peking University, Beijing 100871, China

16 <sup>e</sup>Faculty of Environmental and Symbiotic Sciences, Prefectural University of Kumamoto, Kumamoto  
17 862-8502, Japan

18  
19 \* Corresponding Author - e-mail: shaoL@cumt.edu.cn (Longyi Shao); dzhang@pu-kumamoto.ac.jp  
20 (Daizhou Zhang)  
21  
22

23 **Highlights**

- 24 1. GDI-engine vehicles emitted a large amount of both primary and secondary organic  
25 aerosols.
- 26 2. Higher contents of organic particles were emitted under hot stabilized running and  
27 hot start states.
- 28 3. Sulfate and secondary organic aerosol formed on the surface of primary particles  
29 after ageing.
- 30 4. Particles aged rapidly by catalyzed acidification under high pollution levels in  
31 Beijing.  
32  
33  
34

35 **Abstract:**

36 Air pollution is particularly severe in developing megacities, such as Beijing,  
37 where vehicles equipped with modern gasoline direct injection (GDI) engines are  
38 becoming one of major sources of the pollution. This study presents the characteristics  
39 of individual particles emitted by a GDI gasoline vehicle and their ageing in a smog  
40 chamber under the Beijing urban environment, as part of the Atmospheric Pollution &  
41 Human Health (APHH) research programme. Using transmission electron microscopy,  
42 we identified the particles emitted from a commercial GDI-engine vehicle running  
43 under various conditions, namely, cold start, hot start, hot stabilized running, idle, and  
44 acceleration states. Our results showed that most of the particles were organic, soot and  
45 Ca-rich ones, with small quantities of S-rich and metal-containing particles. In terms of  
46 particle size, the particles exhibited a bimodal distribution in number vs size, with one  
47 mode at 800–900 nm, and the other at 140–240 nm. The amounts of organic particles  
48 emitted under hot start and hot stabilized states were higher than those emitted under  
49 other conditions. The amount of soot particles was higher under cold start and  
50 acceleration states. Under the idle state, the proportion of Ca-rich particles was highest,  
51 although their absolute number was low. In addition to quantifying the types of particles  
52 emitted by the engine, we studied the ageing of the particles during 3.5 hours of  
53 photochemical oxidation in an environmental chamber under the Beijing urban  
54 environment. Ageing transformed soot particles into core-shell structures, coated by  
55 secondary organic species, while the content of sulfur in Ca-rich and organic particles  
56 increased. Overall, the majority of particles from GDI-engine vehicles ~~are~~were organic

57 and soot particles with submicron or nanometric size. The particles ~~are~~were highly  
58 reactive; they reacted in the atmosphere and changed their morphology and composition  
59 within hours via catalyzed acidification that involveds gaseous pollutants at high  
60 pollution levels in Beijing.

61

## 62 **1. Introduction**

63 Air pollution caused by PM<sub>2.5</sub> in megacities such as Beijing, the capital city of  
64 China, is of public and academic concerns due to its environmental impacts (Bond et  
65 al., 2013; Huang et al., 2014; Liu et al., 2017) and adverse health effects (Chart-asa and  
66 Gibson, 2015; Shao et al., 2017). Motor vehicle emissions are one of the most  
67 significant sources of airborne particles in the urban atmosphere (Hwa and Yu, 2014),  
68 and contribute up to 31% of primary particulate emissions of PM<sub>2.5</sub> in Beijing (Yu et  
69 al., 2013). Moreover, secondary aerosol formation associated with traffic emissions is  
70 a major process leading to the rapid increase of PM<sub>2.5</sub>, which results in severe haze  
71 episodes (Huang et al., 2014). Although emissions from gasoline engines are relatively  
72 lower than those from diesel engines (Alves et al., 2015), the number of gasoline-  
73 powered vehicles in urban areas greatly exceeds that of diesel-powered vehicles. The  
74 total number of vehicles in China reached 310 million in 2017, about 70% of these were  
75 powered by gasoline engines (National Bureau of Statistics of China, 2018). There are  
76 two main types of gasoline engines, namely, conventional multipoint port fuel injection  
77 (PFI) engines and gasoline direct injection (GDI) engines. In recent years, the demand  
78 for engines with high efficiency and low fuel consumption has led to an increasing use



79 of GDI engines in light-duty passenger cars. The market share of GDI-engine vehicles  
80 has increased dramatically over the past decade and was estimated to reach 50% of new  
81 gasoline vehicles sold in 2016 (Zimmerman et al., 2016). In Beijing and northern China,  
82 the vehicle emissions become a more concerning issue in terms of air pollution when  
83 the emission from coal combustion are seriously reduced after the Action for  
84 Comprehensive Control of Air Pollution in Beijing since 2017 (Chang et al., 2019;  
85 Chen et al. 2019; Zhang et al. 2019). In spite of this, regional transport of coal-burning  
86 emissions from the surrounding areas can still influence the urban air sometimes  
87 severely in winter (Ma et al., 2017; Zhang et al., 2019).

88 The number, mass and size distribution of particles emitted from GDI-engine  
89 vehicles have been studied (Khalek et al., 2010; Maricq et al., 2011; Baral et al., 2011).  
90 The size distribution usually has an accumulation mode with the maxima in the  
91 diameter range of 100–300 nm. Major components of the particles include elemental  
92 carbon (EC), organic carbon, and ash (Giechaskiel et al., 2014). Besides particulate  
93 matter, the engines emit gaseous hydrocarbon compounds. These compounds might  
94 form particles, or be adsorbed on the surface of particle aggregates, leading to the  
95 growth of the particles in the engine emission (Luo et al., 2015). Relatively high particle  
96 emissions by GDI-engine vehicles have prompted studies on the effects of engine  
97 operating parameters and fuel composition on the characteristics of the particles (Hedge  
98 et al., 2011; Szybist et al., 2011). It has been found that, in general, emissions under the  
99 cold start condition make up the major contribution to the total amount of PM emissions  
100 from GDI engines (Chen and Stone, 2011). Studies have also demonstrated that the

101 highest particle emissions from GDI engines in number concentration occur under the  
102 acceleration state during transient vehicle operations (Chen et al., 2017).

103 Studies have also shown that gasoline vehicles are an important source of  
104 secondary aerosol precursors in urban areas (Suarez-Bertoa et al., 2015). Secondary  
105 aerosols can be formed via gas-phase reactions of volatile organic compounds and  
106 multiphase and heterogeneous processes of primary particles (Zhu et al., 2017).  
107 Experiments performed in environmental chambers demonstrated that the mass of  
108 secondary aerosols derived from precursors could exceed that of directly-emitted  
109 aerosols (Jathar et al., 2014). The occurrence of secondary aerosols on particles could  
110 change the properties of particles in size, mass, chemical composition, morphology,  
111 optical and hygroscopic parameters. These changes, in turn, might affect the  
112 environmental impact of the particles significantly, for instance in terms of visibility,  
113 human health, weather, and energy budgets (Laskin et al., 2015; Peng et al., 2017). In  
114 general, the ageing processes of primary particles in the atmosphere are studied to  
115 understand their climate effects (Niu et al., 2011). However, the lack of data on primary  
116 particles emitted by gasoline engines hinders a deep understanding of the roles and  
117 activities of the particles in ambient air pollution and relevant environmental effects.

118 Atmospheric Pollution & Human Health (APHH) research programme aimed to  
119 explore the sources and processes affecting urban atmospheric pollution in Beijing.  
120 Details regarding this project are given in Shi et al. (2018). To address one of the aims  
121 of the AIRPOLL-Beijing (Source and Emissions of Air Pollutants) and AIRPRO-  
122 Beijing (The integrated Study of AIR Pollution Processes), we employed a dedicated

123 experiment to investigate the characteristics of the individual particles, in terms of the  
124 number concentration, size distribution, emitted from a GDI-engine vehicle during a  
125 real-world driving cycle for chassis dynamometer test, i.e., the Beijing driving cycle  
126 (BDC). Various test modes were introduced to accurately evaluate the emission from  
127 light- or medium-duty vehicles. Furthermore, experiments were conducted in an  
128 environmental chamber to investigate the ageing processes of particles emitted by GDI-  
129 engine vehicles in ambient air in Beijing. We utilized a transmission electron  
130 microscope equipped with an Oxford energy-dispersive X-ray spectrometer (TEM-  
131 EDX) to identify the morphology, size and elemental composition of particles emitted  
132 by the GDI-engine vehicle when it was running under different states. Particles before  
133 and after a 3.5-hour ageing in the chamber were compared on the basis of the TEM-  
134 EDX analysis. The TEM-EDX analysis provides the information on the internal  
135 inhomogeneity, mixing state and surface characteristics of individual particles and has  
136 been used to analyze the aerosol particles (Li and Shao, 2009; Loh et al., 2012; Adachi  
137 and Buseck, 2015; Shao et al., 2017). The experimental design allows for the study of  
138 the physical and chemical characteristics of the particles emitted from the GDI-engine  
139 vehicles, as well as their ageing in a simulated urban atmosphere. The purposes of this  
140 study are to evaluate the individual characteristics and the ageing process of primary  
141 particles emitted by a GDI-engine vehicle, to investigate the ageing processes of such  
142 particles in the atmosphere, and to deepen the understanding of the environmental  
143 impact of gasoline-powered vehicle emissions.

## 144 **2. Material and methods**

### 145 **2.1 Test vehicle, fuels, and test procedure**

146 The GDI-engine vehicle utilized in the experiment complies with the China Phase  
147 4 (equivalent to Euro 4) standard. It uses a three-way catalyst to reduce gaseous  
148 emissions. The GDI (model GDI-1.4-T) in the test vehicle is recognized as a  
149 representative of leading-edge designs of gasoline engines, because of its advanced  
150 engine technologies such as its better fuel burning efficiency and lower greenhouse gas  
151 emissions than other types of engine. Vehicles equipped with such GDI engines  
152 constitute the majority of light-duty vehicles in China, especially in large cities like  
153 Beijing. Details of the engine used in this study are listed in Table S1. The fuel used in  
154 the experiment is a commercial gasoline blend of common quality in China. The  
155 properties of the fuel were measured by SGS-CSTC Standards Technical Services Co.,  
156 Ltd., China, and are listed in Table S2. The fuel has a Research Octane Number (RON)  
157 of 93 and is a fifth-stage gasoline. It contains 36.7% of aromatics and 15.4% of olefins  
158 in volume and has 6% of sulfur in mass, representing a typical fifth-stage gasoline in  
159 China (with high aromatics) and is now widely used in Beijing. The experiments were  
160 conducted within repeated Beijing Driving Cycles (BDCs), and one BCD included a  
161 200-s “cold start” phase followed by an 867-s “hot stabilized running” phase. The  
162 conditions during a BDC in the experiments are illustrated in Figure S1a. The cold start  
163 state was achieved by starting the vehicle with a period of small accelerations, while  
164 the hot stabilized running state had multiple periods of large acceleration and a  
165 maximum velocity of 50 km h<sup>-1</sup>. The BDC, characterized by a higher proportion of  
166 idling periods and a lower acceleration speed than the New European Driving Cycle

167 (NEDC), was performed to simulate the repeated braking and acceleration on road in  
168 megacities such as Beijing.

169 All tests were performed on a Euro 5/LEV2/Tier 2-capable test cell on a 48-inch  
170 single-roll chassis dynamometer at the State Key Laboratory of Automobile Safety and  
171 Energy Conservation at Tsinghua University. The test procedure for each run was as  
172 follows: fuel change, BDC preparation, soak, cold start BDC test, and hot start BDC  
173 test. After fuel change and BDC preparation, the test vehicle was then conditioned with  
174 an overnight soak for more than 10 h. The soak room temperature was maintained  
175 between 20 and 30 °C. Due to the limitation of the facilities and available running time,  
176 a hot start test was conducted within 5 mins after the cold start test. A dilution unit was  
177 applied to dilute the exhaust from the tailpipe into 1/10 in volume using synthetic air  
178 composed of 79% N<sub>2</sub> and 20% O<sub>2</sub>, in order to obtain the concentrations suitable for  
179 subsequent measurements and suppress possible coagulation. The number  
180 concentration of the emitted particles was monitored by a Combustion Fast Particle  
181 Size Spectrometer Differential Mobility Spectrometer 500 (DMS 500). The maximum  
182 measurable number concentration of DMS 500 was 10<sup>11</sup> (dN/dlogDp/cc) after the  
183 dilution (Petzold et al., 2011). For the analyses of individual particles, 6–8 samples  
184 were collected during one BDC test. At least one sample was collected under each  
185 running state (i.e. cold start, hot start, idle state, acceleration state, or hot stabilized  
186 running state). The driving cycle test was repeated at least twice. Two or more samples  
187 were obtained for each running state. A single-stage cascade impactor (KB-2, Qingdao  
188 Jinshida Company) was mounted to the exit of the tailpipe after the dilution unit. The

189 emitted particles were collected onto 300-mesh copper TEM grids, which were covered  
190 with a carbon-coated formvar film. The flow rate was  $1.0 \text{ L min}^{-1}$ , and the cut-off  
191 diameter of the impactor for 50% collection efficiency was  $0.25 \mu\text{m}$  if the density of  
192 the particles was  $2 \text{ g cm}^{-3}$ . For each sample, the collection time was 60 s.

## 193 2.2 Environmental chamber experiments

194 Particles from the GDI-engine vehicle were introduced into an environmental  
195 chamber and exposed to sunlight. The chamber, made of perfluoroalkoxy (PFA) Teflon  
196 in order to achieve a high transmission of ultraviolet light, ~~had~~ has an internal volume  
197 of  $1.2 \text{ m}^3$ . Ambient sunlight was used as the driving force for photochemical reactions  
198 in the chamber, in an environment close to actual open air. Before the experiments, the  
199 chamber was cleaned by flushing with zero air for approximately 12 hours and  
200 illuminated with sunlight, to remove residues that could influence the experiments.

201  $\text{H}_2\text{O}_2$  (1 mL, 30%), together with the vehicle emission, was injected into the chamber  
202 to generate OH exposure. The OH exposure at the end of the experiments reproduced  
203 extreme oxidation processes, which were equivalent to cases of an oxidation more than  
204 10 days in Beijing ambient air if the 24-hour-mean concentration of OH is  $10^6$   
205 molecules  $\text{cm}^{-3}$  (Lu et al., 2013). ~~Assuming the 24 hr mean concentration of  $10^6$  OH~~  
206 ~~molecules  $\text{cm}^{-3}$  in Beijing (Lu et al., 2013), the OH exposure at the end of the~~  
207 ~~experiments reproduced extreme oxidation processes in the atmosphere, which is~~  
208 ~~equivalent to cases of an oxidation more than 10 days~~ The aging experiments for the

209 gasoline exhausts were carried out with a relatively high OH exposure compared to  
210 ambient conditions in order to obtain the aging process. This method and the amount  
211 of  $\text{H}_2\text{O}_2$  have been frequently used in smog chamber experiments (Song et al., 2007;

带格式的: 上标

带格式的: 上标

212 Song et al., 2019). After the injection, the experiments were conducted from  
213 approximately 13:00 to 17:00 local time under sunshine, with the relative humidity  
214 being kept at around 50%. The global solar radiation when the tests were carried out  
215 was approximately  $318 \text{ W m}^{-2}$ . After 3.5 h of ageing, the particles in the chamber were  
216 collected onto mesh TEM grids using the impactor. The collection time for each sample  
217 was 120 s. The schematic diagram of the experimental system is presented in Figure  
218 S1b.

219

### 220 **2.3 TEM/EDX and scanning transmission electron microscopy (STEM) analyses**

221 The particles in the samples were examined using a Tecnai G2 F30 field emission  
222 high-resolution transmission electron microscope (FE-HRTEM). This microscope is  
223 also equipped with an Oxford EDX and a STEM unit with a high-angle annular dark-  
224 field detector (HAADF). The EDX can detect elements with the atom number larger  
225 than 5 (B) in a single particle. The HAADF can detect the distribution of a certain  
226 element by mapping the distribution of the element in a particle. The TEM was operated  
227 with the acceleration voltage of 300 kV. EDX spectra were firstly collected for 20 live  
228 seconds to minimize the influence of radiation exposure and potential beam damage  
229 and then for 90 live seconds for a range of possible elements. Copper was excluded  
230 from the analysis because of interference from the TEM grids which ~~are~~were made of  
231 copper.

232 To ensure the representativeness of the analyzed particles, more than 150 particles  
233 from at least 3 random areas were analyzed from the center and periphery of the  
234 sampling spot on each grid. All individual particles larger than 50 nm in the selected

235 areas were analyzed. The TEM images were digitized using an automated fringe image  
236 processing system named Microscopic Particle Size of Digital Image Analysis System  
237 (UK) to project the surface areas of the particles. The equivalent spherical diameter of  
238 a particle was calculated from its projected area, expressed as the square root of  $4A/\pi$ ,  
239 where A ~~is~~-was the projected area. The electron microscope analysis of individual  
240 particles ~~is~~-was very time consuming, which hindered us from analyzing more particles  
241 from multiple engines emission. There are differences in emissions from vehicles to  
242 vehicles, even for vehicles with same model engines. Only one GDI vehicle, the type  
243 of which constitutes the majority of light-duty vehicles in China, was tested in this study.  
244 The representativeness of the present results remains unevaluated carefully with, such  
245 as, comparisons between vehicles to achieve broader statistical results, although the  
246 tests in the present studies were conducted under strict control conditions.

### 247 **3. Results**

#### 248 **3.1. Particle morphology, elemental composition and size**

249 A total of 2880 particles were analyzed from the GDI-engine vehicles. Most of the  
250 particles were in the sub-micrometer size range. Based on morphology and elemental  
251 composition of the particles, the majority of them were identified as soot, organic and  
252 Ca-rich particles, a smaller amount was identified as S-rich or metal-rich particles (Fig.  
253 1). The method of particle classification is similar to that adopted by Okada et al. (2005)  
254 and Xing et al. (2019). In the following description, “X-rich” means that the element  
255 “X” occupies the largest proportion in the element composition of the particles. Figure  
256 2 illustrates the number-size distributions of the relative concentration ( $dN/d\log D$ ) of  
257 primary particles from the GDI-engine vehicle, where N is the relative number fraction



258 and D is the equivalent diameter. The particles were in the range of 60–2500 nm and  
259 displayed a bimodal distribution, with one mode in the 140–240 nm range, and another  
260 in the 800–900 nm range. Particles smaller than 250 nm were largely underestimated  
261 because of the loss during the particle collection. Therefore, there should have been  
262 more particles in the smaller mode range than shown in Figure 2. Concerning the loss  
263 of small particles, we measured the size distribution by the DMS500 (Fig. S2). The  
264 results showed that a large amount of nucleation mode particles were emitted by the  
265 GDI vehicle.

266 It should be noted that organic particles were mainly composed of C and O  
267 elements, and contained a small amount of inorganic elements Ca, P, S and Zn.  
268 Elemental mapping of the organic particles exhibited the presence of Ca, P, S and Zn in  
269 some of the particles, showing the mixture state of organic and inorganic materials (Fig.  
270 1f). It has been reported that such particles could be related to the combustion of fuels  
271 or lubrication oil (Rönkkö et al., 2013). In addition to these primary organic particles,  
272 the GDI-engine vehicle emitted precursor gases, which produced secondary organic  
273 particles via gas-phase reactions, and multiphase and heterogeneous processes on the  
274 primary particles. A group of spherical particles were found in the environmental  
275 chamber (Fig. 1g). These particles became semi-transparent or transparent to an  
276 electron beam, which ~~is~~was characteristic of organic materials, liquid water, or their  
277 evaporation residues either mixed or not mixed with electron absorptive materials. We  
278 regarded these particles as secondary organic particles because the humidity in the  
279 chamber during the experiment was kept much below saturation (relative humidity

280 around 50%). Therefore, these particles were expected to mainly consist of secondary  
281 organic materials, which should have been produced via gas phase reactions or on the  
282 surface of pre-existing particles (Hu et al., 2016). No other elements, except C and O,  
283 were identified in these particles, which ~~is~~was consistent with the above inference.  
284 Similar particles were also encountered in other environmental chamber experiments  
285 studying emissions from light-duty gasoline vehicles (Jathar et al., 2014).

286

### 287 3.2 Number fractions of particles

288 Figure 3 illustrates the numbers of accumulation mode particles emitted by  
289 burning one kilogram of fuel during the cold start and hot start driving cycles. PM  
290 emissions at the start-up stage under both cold and hot start states were higher than the  
291 emissions under the states when the engine was fully warmed and the vehicle operation  
292 was stabilized. The PM emission was the highest under the hot stabilized running state  
293 ( $2.3 \times 10^{10}$  particles (kg fuel)<sup>-1</sup>), followed by those under the hot start ( $1.2 \times 10^{10}$  particles  
294 (kg fuel)<sup>-1</sup>), cold start ( $7.1 \times 10^9$  particles (kg fuel)<sup>-1</sup>), and acceleration running states  
295 ( $2.9 \times 10^9$  particles (kg fuel)<sup>-1</sup>), with the emission under the idle running state being the  
296 lowest ( $7.4 \times 10^8$  particles (kg fuel)<sup>-1</sup>) (Fig. S3). The higher emission of particle in term  
297 of number for the GDI vehicle under the hot start state can be ascribed to the  
298 experimental time of the vehicle engine. The hot start test in this study was conducted  
299 within 5 mins after the cold start test. The PM emissions from GDI vehicles were  
300 relatively less affected by ambient temperature for the initial 30 minutes during the  
301 warming up of the engines (Cotte et al., 2001). This may lead to the high value of the  
302 PM emission for the hot start state which is slightly higher than that for the cold start

303 state. Although the total PM emission were higher under hot start state than that under  
304 the cold start state, the comparison of those in the size range of accumulation mode  
305 indicates that the particulate emissions for this mode of particles were higher under the  
306 cold start state than under the hot start sate (Fig. 3). This can be attributed to the less  
307 efficiency of the vaporization of fuel droplets in the combustion cylinder under the cold  
308 start state (Chen et al., 2017). Size distributions of the particles varied with driving  
309 conditions (Fig. S4). Under the cold start state and acceleration running state, higher  
310 number concentrations, and thus higher mass concentrations of the particles with  
311 accumulation mode were emitted in comparison with other running states.

312 Under all the running states, morphologies and types of the particles remained  
313 similar but the proportions of different types of particles differed considerably (Fig. S5).  
314 The proportion of organic particles was high under hot stabilized and hot start states.  
315 Soot particles were abundant under cold start and acceleration states. A relatively higher  
316 proportion of Ca-rich particles was found under idle state, compared to those under  
317 other running states.

318 We estimated the number of different type particles in the emission under the  
319 running states by burning one kilogram of fuel (Fig. 4). Organic particles in the  
320 emission under the hot stabilized running state ( $2.3 \times 10^9$  particles (kg fuel)<sup>-1</sup>) and the  
321 hot start running state ( $3.6 \times 10^8$  particles (kg fuel)<sup>-1</sup>) were higher than in the emission  
322 under other running states. The number of soot particles were higher under the hot  
323 stabilized running state ( $1.7 \times 10^9$  particles (kg fuel)<sup>-1</sup>) and the cold start state ( $5.9 \times 10^8$   
324 particles (kg fuel)<sup>-1</sup>) than those under other running states. Under the idle state, the

325 relative proportion of Ca-rich particles was the highest, although their absolute number  
326 was low ( $1.4 \times 10^9$  particles (kg fuel)<sup>-1</sup>).

327 Under the cold start state, a significant proportion of the emitted particles were  
328 soot particles. This can be attributed to the incomplete vaporization of fuel droplets in  
329 the combustion cylinder (Chen et al., 2017). Under the hot start state and the hot  
330 stabilized running state, organic particles were predominant. Under these two running  
331 states, the engine temperature was high, which enabled the fuel to evaporate and mix  
332 with the air easily. With the increase of the temperature in the cylinders, the rate of  
333 particle oxidation increased, which could cause an increase of organic particles in the  
334 emission (Fu et al., 2014). Under the idle state, the fuel consumption was much lower  
335 than that under the other running states, which resulted in a higher relative contribution  
336 to particles from lubricant oil. The high Ca content in the lubricant oil led to a higher  
337 Ca-rich particle emission under this running state. Under the acceleration state, the  
338 predominant types of particle included soot, organic, and Ca-rich particles. As the  
339 acceleration running required a high vehicular speed and engine load, the emissions  
340 contained more soot particles than those under other running states.

### 341 **3.3. Aged particles in the environmental chamber**

342 A large amount of secondary organic particles (accounting for 80%-85% in  
343 number), some soot particles, Ca-rich particles, and primary organic particles were  
344 detected in the environmental chamber (Fig. 5). After the ageing process, many soot  
345 particles changed into core-shell structures and became coated with secondary species  
346 (Figs. 5b and 5c). The EDX results showed that almost all coatings were mainly  
347 composed of C, O, and S, suggesting these coatings were a mixture of organic and

348 sulfate. The morphology and compositions of Ca-rich particles and organic particles  
349 (Figs. 5e and 5g) changed, with the aged ones having a more irregular shape and a  
350 higher sulfur content in comparison with fresh ones (Figs. 5A and B).

351        Approximately 80% of the soot particles were present in core-shell structures and  
352 coated with secondary species after the 3.5-hour ageing. In contrast, before the ageing,  
353 the particles with a core-shell structure were only about 10% of the total. The mean  
354 diameter of the soot particles after ageing was around 0.49  $\mu\text{m}$ , which was much smaller  
355 than that before the ageing (0.65  $\mu\text{m}$ ), indicating the shrinkage of the soot particles  
356 during the ageing (Fig. 5b). The core-shell ratios, defined as the ratio of the diameter of  
357 the core part ( $D_{\text{core}}$ ) to the diameter of the whole particle ( $D_{\text{shell}}$ ) (Niu et al., 2016;  
358 Hou et al., 2018), were used to quantify the aging degree of the soot particles with  
359 coating. It was found that the core-shell ratios of the soot particles in the smog chamber  
360 were mainly in the range of 0.25–0.78, indicating the stronger aging degree of soot  
361 particles in the chamber than case data in urban air with the ratios of 0.4–0.9 (Niu et al.,  
362 2016).”

## 363 **4. Discussion**

### 364 **4.1. Contribution of GDI-engine vehicle emissions to urban air pollution**

365        Our investigation ~~shows~~showed that the GDI-engine vehicle emitted a large  
366 amount of organic particles (32%), soot (32%), Ca-rich particles (26%), S-rich (5%)  
367 and metal-containing particles (4%). Relevant studies have also shown that the primary  
368 carbonaceous aerosols (element carbon + primary organic aerosol) accounted for 85 %  
369 of the PM in the GDI vehicles, suggesting that carbonaceous aerosols were the major

370 contributors in the PM from GDI gasoline vehicles (Du et al., 2018). Considering the  
371 large fraction of the vehicles equipped with GDI engines in megacities like Beijing, this  
372 indicates a possible substantial contribution of GDI-engine vehicles to urban air  
373 pollution. Moreover, organic particles occupied the majority of the particles emitted  
374 under hot stabilized running and hot start states. It has been noted that the organic matter  
375 was the major component of the total particle mass during the hot start conditions  
376 (Fushimi et al., 2016; Chen et al., 2017), which ~~is~~was consistent with the results  
377 obtained for the number concentrations in our study. The hot stabilized running state is  
378 the most frequent running condition of vehicles, whereas the hot start state is the most  
379 frequent condition in congested traffic. This suggests that a substantial number of  
380 organic compounds in the air pollution of populated cities might be directly related to  
381 vehicle emissions.

382       Organic particles and soot particles in ambient air are emitted from a range of  
383 sources including fossil fuels, biomass burning and urban waste burning (Kanakidou et  
384 al., 2005). Table 1 shows the major characteristics of particles in the emissions from  
385 different sources. For instance, there is a higher fraction of soot particles and a lower  
386 fraction of organic particles in the emissions of GDI-engine vehicles compared to PFI-  
387 engine vehicles (Xing et al., 2017). Organic particles in emissions from gasoline  
388 vehicles are usually enriched in Ca, S and P (Xing et al., 2017; Liati et al., 2018). In  
389 comparison, emissions from biomass/wood burning are usually dominated by organic  
390 particles, which account for more than 50% of the total amount of particles (Liu et al.,  
391 2017). Furthermore, organic particles from biomass/wood burning usually show

392 elevated K content, and thus, this element is frequently used as an indicator for  
393 biomass/wood burning organic particles (Niu et al., 2016). Observations of primary  
394 particles directly from coal burning have also demonstrated a predominance of organic  
395 particles, soot particles, S-rich particles and mineral particles (Zhang et al., 2018; Wang  
396 et al., 2019). Both biomass burning and coal combustion can produce organic particles  
397 and almost all the emitted particles contain a certain amount of Si in addition to C and  
398 O. Table 1 also shows the elemental concentrations in the organic particles in the  
399 emissions from different types of sources. Since the concentrations of minor elements  
400 in the organic particles are highly dependent on the sources, they could be used for  
401 source identification of individual particles in the atmosphere.

402 The present data also permit the compilation of a rough inventory of particle  
403 categories and amounts emitted from GDI-engine vehicles under various running  
404 conditions (Fig. 4). Combined with statistics on the number of vehicles with GDI  
405 engines, the running time and the running conditions on roads within a certain area, it  
406 is possible to make an approximate estimate of the amounts of primary particles emitted  
407 from GDI-engine vehicles. Such estimate is the basis for accurate source apportionment  
408 of particles from vehicles, and it will be very beneficial for studies on the anthropogenic  
409 sources of primary particles in urban air. These data could be brought together to better  
410 understand the sources of air pollutants in the Beijing megacity and to improve the  
411 capability of developing cost-effective mitigation measures.

#### 412 **4.2 Rapid ageing of primary particles in Beijing**

413 The results of chamber experiments indicate that sulfate and secondary organic

414 aerosol (SOA) form on the surface of soot, Ca-rich and organic particles. Moreover, the  
415 atmospheric transformation of primary particles emitted by the GDI-engine vehicles  
416 could occur within 3.5 hours, indicating the ageing was rapid. Peng et al. (2014) found  
417 similar timescales for black carbon transformation under polluted conditions in Beijing.  
418 The rapid ageing of primary particles could be caused by several factors, such as the  
419 concentration of gaseous pollutants from the vehicles, strength of solar radiation,  
420 relative humidity (RH), and O<sub>3</sub> concentration (Guo et al., 2012; Deng et al., 2017; Du  
421 et al., 2018). The present experiments were conducted in the atmosphere with relative  
422 humidity of approximately 50% and solar radiation of 318 Wm<sup>-2</sup>. The total hydrocarbon  
423 emission (THC) from the GDI vehicles was 0.297 g km<sup>-1</sup>. Repeated braking and  
424 acceleration in the BDC could cause incomplete combustion and consequently high  
425 THC emission. Under a high concentration of gaseous pollutants, primary particles  
426 would age rapidly when exposed to solar radiation. Consequently, secondary species  
427 including SOA and sulfate were produced on or condensed onto the particles, leading  
428 to the coating. Guo et al. (2014) also showed that secondary photochemical growth of  
429 fine aerosols during the initial stage of haze development could be attributed to highly  
430 elevated levels of gaseous pollutants.

431       The mixture of SOA and sulfate have been detected in our chamber experiment,  
432 indicating the involvement of inorganic salts in the SOA formation. Previous studies  
433 have demonstrated the enhancement of SOA production in the presence of inorganic  
434 sulfate (Beardsley and Jang, 2015; Kuwata et al., 2015), and this is because sulfate can  
435 catalyze carbonyl heterogeneous reactions, and consequently, lead to SOA production



436 (Jang et al., 2002; Jang et al., 2004). Moreover, these aged primary particles favored  
437 the formation of secondary aerosols by providing reaction sites and reaction catalysts.  
438 Sulfate and secondary organic aerosol (SOA) co-existed on the surface of primary  
439 particles, such as soot, Ca-rich and organic particles. In addition, the products of VOCs  
440 oxidation could react with SO<sub>2</sub> to rapidly produce sulfate (Mauldin et al., 2012). Thus,  
441 the rapid ageing of primary particles could also be attributable to the acid-catalyzed  
442 mechanism. As the major source of pollutants in urban air, the GDI-engine vehicles  
443 supply both primary particles and precursor gaseous species, and the rapid ageing of  
444 the particles under certain conditions is very likely to be the major driving force for the  
445 elevation of urban air pollution.

#### 446 **4.3 Implications and perspectives**

447 Our results indicated ~~ed~~ that GDI-engine vehicles emitted a large amount of both  
448 primary and secondary organic aerosols. PM number emission of organic particles from  
449 GDI-engine vehicle were  $2.9 \times 10^9$  particles (kg fuel)<sup>-1</sup> during the BDC. Secondary  
450 organic particle was predominant in the secondary aerosols, accounting for 80-85%  
451 particles in the chamber. Organic aerosols (OA) play an important role in the Earth's  
452 radiation balance not only for its absorption and scattering of solar radiation but also  
453 because they can alter the microphysical properties of clouds (Scott et al., 2014).  
454 Particle size, shape, mixing state and composition affect their light scatterings and  
455 absorption cross sections, and cloud condensation nuclei activity (Jacobson, 2001). OA  
456 ~~were-are~~ composed of various types of chemical compounds with varying absorption  
457 properties (mixing state), which ~~were-are~~ determined by the emission sources, the

458 formation mechanism (Zhu et al., 2017), and the source regions (Laskin et al., 2015).  
459 Primary OA from biomass burning ~~was~~is co-emitted with soot (black carbon),  
460 inorganic salts, and fly ash, producing internally and externally mixed particles in  
461 which the organic components ~~were~~are present in different relative abundance (Lack  
462 et al., 2012). Similarity, primary OA in the exhaust of gasoline and diesel vehicles ~~were~~  
463 are mixed with Ca, P, Mg, Zn, Fe, S, and minor Sn inorganic compounds (Liati et al.,  
464 2018). In addition, previous measurements have indicated that SOA usually exists as  
465 an internal mixture with other aerosols, such as sulfate, ammonium, or nitrate (Zhu et  
466 al., 2017). Our results showed that the POA emitted from GDI-engine vehicle were  
467 mixed with soot, inorganic components such as Ca, P, and Zn. Some of the SOA formed  
468 in the smog chamber were mixed with sulfate. The complexity of mixing state makes it  
469 difficult to characterize the properties of OA. Lang-Yona et al. (2010) have found that  
470 for aerosols consisting of a strongly absorbing core coated by a non-absorbing shell,  
471 ~~and~~ the Mie theory prediction deviated from the measurements by up to 10%. Moreover,  
472 atmospheric aging process, involving aqueous-phase aging and atmospheric oxidation,  
473 can either enhance or reduce light absorption by OA (Bones et al., 2010). The  
474 condensation process may result in a dramatic enhancement of hydrolysis of OA  
475 compounds, affecting their absorption spectra (Lambe et al., 2015).

476 Our results also showed that primary organic aerosols (POA) emitted by GDI-  
477 engine vehicles could acquire OA and sulfate coatings rapidly, within a few hours, and  
478 increase a sizable fraction of total ambient aerosols existing as internal mixtures. In  
479 addition, the fast ageing further caused the increase of aged POA in the total OA,

480 consequently, largely modified the properties of the particles such as their optical  
481 properties. The results of the experiments in the chamber showed that most of the aged  
482 POA had a core-shell structure, whereas most of the secondary organic aerosols (SOA)  
483 produced by gas-phase reactions had a uniform structure. These results push forward  
484 the understanding on the mixing state and chemical composition of both POA and SOA.  
485 The experimental data will benefit the parameterization of vehicles emissions in  
486 numerical models dealing with urban air pollution.

## 487 5. Conclusions

488

- 489 1. Five types of individual particles emitted by a GDI-engine gasoline vehicle~~the~~  
490 ~~GDI-engine vehicles~~ were identified, including soot, organic, Ca-rich, S-rich, and  
491 metal-rich particles. Among them, soot, organic, and Ca-rich particles were  
492 predominant. The particles emitted from ~~GDI-engine vehicles~~this commercial  
493 GDI-engine gasoline vehicle displayed a bimodal size distribution.
- 494 2. The concentrations of the particles emitted by this commercial GDI-engine  
495 gasoline vehicle~~the GDI-engine vehicles~~ vary with different running conditions.  
496 The PM emission was the highest under the hot stabilized running state, followed  
497 by those under the hot start, cold start, and acceleration running states, with the  
498 emission under the idle running state being the lowest under the idle running state.
- 499 3. The relative proportions of the different types of particles emitted by this  
500 commercial GDI-engine gasoline vehicle~~the GDI-engine vehicles~~ vary-varied with  
501 different running conditions. Large amounts of organic particles were emitted  
502 during hot stabilized and hot start states. Under cold start and acceleration states,

503 the emissions were enriched in soot particles. Under idle state, a relatively higher  
504 number of Ca-rich particles was emitted, although the absolute number was low.

505 4. After ageing in the environmental chamber, the structure of the soot particles  
506 changed into a core-shell structure, and the particles were coated with condensed  
507 secondary organic material. Ca-rich particles and organic particles also were  
508 modified, and their content of sulfur increased after ageing.

509 5. Ageing of the emitted particles occurred rapidly, within hours. Such rapid ageing  
510 could be attributable to an acid-catalyzed mechanism and to the high initial  
511 concentrations of gaseous pollutants emitted by [this commercial GDI-engine](#)  
512 ~~gasoline vehicle~~ ~~the GDI engine~~ ~~gasoline~~.

513

#### 514 **Data availability**

515 All data presented in this paper are available upon request. Please contact the  
516 corresponding author (shaoL@cumtb.edu.cn).

#### 517 **Author contribution**

518 LS designed this study; JX performed the experiments. JX, LS, DZ summarized  
519 the data and wrote the paper. WZ, JP, WW, SS, MH supported the experiments and  
520 commented the paper.

#### 521 **Competing interests**

522 The authors declare that they have no conflict of interest.

#### 523 **Acknowledgements**

524 This work was supported by Projects of International Cooperation and Exchanges

525 NSFC (Grant No. 41571130031). The data analysis was partly supported by Science  
526 and Technology Project Founded by the Education Department of Jiangxi Province (No.  
527 GJJ180226), Yue Qi Scholar Fund of China University of Mining and Technology  
528 (Beijing), and a Grant-in-Aid for Scientific Research (B) (No.16H02942) from the  
529 JSPS.

## 530 **References**

- 531 Adachi, K., and Buseck, P. R.: Changes in shape and composition of sea-salt particles upon aging in an  
532 urban atmosphere, *Atmos. Environ.*, 100, 1-9, <http://dio.org/10.1016/j.atmosenv.2014.10.036>, 2015.
- 533 Alves, C. A., Lopes, D. J., Calvo, A. I., Evtyugina, M., Rocha, S., and Nunes, T.: Emissions from light-  
534 duty diesel and gasoline in-use vehicles measured on chassis dynamometer test cycles, *Aerosol Air*  
535 *Qual. Res.*, 15(1), 99-116, <http://dio.org/10.4209/aaqr.2014.01.0006>, 2015.
- 536 Baral, B., Raine, R., and Miskelly, G.: Effect of engine operating conditions on spark-ignition engine  
537 PAH emissions, SAE Technical Paper 2011-01-1161, <http://dio.org/10.4271/2011-01-1161>, 2011.
- 538 Beardsley, R.L., and Jang, M.: Simulating the SOA formation of isoprene from partitioning and  
539 aerosol phase reactions in the presence of inorganics, *Atmos Chem Phys*, 15, 33121-33159,  
540 <http://dio.org/10.5194/acpd-15-33121-2015>, 2015.
- 541 Bond, T. C., Doherty, S. J., Fahey, D. W., Forster, P. M., Berntsen, T., DeAngelo, B. J., Flanner, M. G.,  
542 Ghan, S., Köhler, B., Koch, D., Kinne, S., Kondo, Y., Quinn, P. K., Sarofim, M. C., Schultz, M.  
543 G., Schulz, M., Venkataraman, C., Zhang, H., Zhang, S., Bellouin, N., Guttikunda, S. K., Hopke, P.  
544 K., Jacobson, M. Z., Kaiser, J. W., Klimont, Z., Lohmann, U., Schwarz, J. P., Shindell, D.,  
545 Storelvmo, T., Warren, S. G., and Zender, C. S.: Bounding the role of black carbon in the climate  
546 system: A scientific assessment, *J. Geophys. Res.-Atmos.*, 118(11), 5380-5552,  
547 <http://dio.org/10.1002/jgrd.50171>, 2013.
- 548 Bones, D.L., Henricksen, D.K., Mang, S.A., Gonsior, M., Bateman, A.P., Nguyen, T.B., Cooper,  
549 W.J., and Nizkorodov, S.A.: Appearance of strong absorbers and fluorophores in limonene-O<sub>3</sub>  
550 secondary organic aerosol due to NH<sup>+</sup>-mediated chemical aging over long time scales, *J*  
551 *Geophys Res*, 115, <http://dio.org/10.1029/2009JD012864>, 2010.
- 552 Chart-asa, C., and Gibson, J. M.: Health impact assessment of traffic-related air pollution at the urban project scale: Influence of  
553 variability and uncertainty, *Sci. Total Environ.*, 506-507, 409-421,  
554 <http://dio.org/10.1016/j.scitotenv.2014.11.020>, 2015.
- 555 Chang, L., Shao, L., Yang, S., Li, J., Zhang, M., Feng, X., Li, Y., 2019, Study on variation characteristics  
556 of PM<sub>2.5</sub> mass concentrations in Beijing after the action for comprehensive control of air pollution.  
557 *Journal of Mining Science and Technology*, 2019, 4(6): 539-546. [http://dio.org/10.](http://dio.org/10.19606/j.cnki.jmst.2019.06.009)  
558 [19606/j.cnki.jmst.2019.06.009](http://dio.org/10.19606/j.cnki.jmst.2019.06.009). (in Chinese with English Abstract)
- 559 Chart-asa, C., and Gibson, J. M.: Health impact assessment of traffic-related air pollution at the urban  
560 project scale: Influence of variability and uncertainty, *Sci. Total Environ.*, 506-507, 409-421,  
561 <http://dio.org/10.1016/j.scitotenv.2014.11.020>, 2015.
- 562 Chen, Z., Chen, D., Xie, X., Cai, J., Zhuang, Y., Cheng, N., He, B., and Gao, B.: Spatial self-aggregation

563 effects and national division of city-level PM<sub>2.5</sub> concentrations in China based on spatio-temporal  
564 clustering, *J. Clean. Prod.*, 207, 875-881, <http://dio.org/10.1016/j.jclepro.2018.10.080>, 2019.

565 Chen, L., Liang, Z., Zhang, X., and Shuai, S.: Characterizing particulate matter emissions from GDI and  
566 PFI vehicles under transient and cold start conditions, *Fuel*, 189, 131-140,  
567 <http://dio.org/10.1016/j.fuel.2016.10.055>, 2017.

568 Chen, L., and Stone, R.: Measurement of enthalpies of vaporization of isooctane and ethanol blends and  
569 their effects on PM emissions from a GDI engine, *Energ. Fuel*, 25(3), 1254-1259,  
570 <http://dio.org/10.1021/ef1015796>, 2011.

571 [Cotte, H., Bessagnet, B., Blondeau, C., Mallet-Hubert, P.Y., Momioue, J.C., Walter, C., Boulanger, L.,  
572 Deleger, D., Jouvenot, G., Pain, C., and Rouveiolles, P.: Cold-start emissions from petrol and diesel  
573 vehicles according to the emissions regulations \(from Euro 92 to Euro 2000\), \*Int J Vehicle Des\*, 27,  
574 275-285, 10.1504/IJVD.2001.001971, 2001.](#)

575 Deng, W., Hu, Q., Liu, T., Wang, X., Zhang, Y., Song, W., Sun, Y., Bi, X., Yu, J., Yang, W., Huang, X.,  
576 Zhang, Z., Huang, Z., He, Q., Mellouki, A., and George, C.: Primary particulate emissions and  
577 secondary organic aerosol (SOA) formation from idling diesel vehicle exhaust in China, *Sci. Total  
578 Environ.*, 593-594, 462-469, <http://dio.org/10.1016/j.scitotenv.2017.03.088>, 2017.

579 Du, Z., Hu, M., Peng, J., Zhang, W., Zheng, J., Gu, F., Qin, Y., Yang, Y., Li, M., Wu, Y., Shao, M., and  
580 Shuai, S.: Comparison of primary aerosol emission and secondary aerosol formation from gasoline  
581 direct injection and port fuel injection vehicles, *Atmos. Chem. Phys.*, 18(12), 9011-9023,  
582 <http://dio.org/10.5194/acp-18-9011-2018>, 2018.

583 Fu, H., Wang, Y., Li, X., and Shuai, S.: Impacts of cold-start and gasoline RON on particulate emission  
584 from vehicles powered by GDI and PFI engines, *SAE Technical Paper 2014-01-2836*, [http://dio.org/  
585 10.4271/2014-01-2836](http://dio.org/10.4271/2014-01-2836), 2014.

586 Fushimi, A., Kondo, Y., Kobayashi, S., Fujitani, Y., Saitoh, K., Takami, A., and Tanabe, K.:  
587 Chemical composition and source of fine and nanoparticles from recent direct injection  
588 gasoline passenger cars: Effects of fuel and ambient temperature, *Atmos Environ*, 124, 77-84,  
589 <http://dio.org/10.1016/j.atmosenv.2015.11.017>, 2016.

590 Giechaskiel, B., Maricq, M., Ntziachristos, L., Dardiotis, C., Wang, X., Axmann, H., Bergmann, A., and  
591 Schindler, W.: Review of motor vehicle particulate emissions sampling and measurement: From  
592 smoke and filter mass to particle number, *J. Aerosol Sci.*, 67, 48-86,  
593 <http://dio.org/10.1016/j.jaerosci.2013.09.003>, 2014.

594 Guo, S., Hu, M., Guo, Q., Zhang, X., Zheng, M., Zheng, J., Chang, C. C., Schauer, J. J., and Zhang, R.:  
595 Primary sources and secondary formation of organic aerosols in Beijing, China, *Environ. Sci.  
596 Technol.*, 18(46), 9846 - 9853, 2012.

597 Hedge, M., Weber, P., Gingrich, J., Alger, T., and Khalek, I. A.: Effect of EGR on Particle Emissions  
598 from a GDI Engine, *SAE Int. J. Engines*, 4(1), 650-666, <http://dio.org/10.4271/2011-01-0636>, 2011.

599 Hou, C., Shao, L., Hu, W., Zhang, D., Zhao, C., Xing, J., Huang, X., and Hu, M.: Characteristics  
600 and aging of traffic-derived particles in a highway tunnel at a coastal city in southern China,  
601 *Sci Total Environ*, 619-620, 1385-1393, <http://dio.org/10.1016/j.scitotenv.2017.11.165>, 2018.

602 Hu, W., Niu, H., Zhang, D., Wu, Z., Chen, C., Wu, Y., Shang, D., and Hu, M.: Insights into a dust event  
603 transported through Beijing in spring 2012: Morphology, chemical composition and impact on  
604 surface aerosols, *Sci. Total Environ.*, 565, 287-298, <http://dio.org/10.1016/j.scitotenv.2016.04.175>,  
605 2016.

606 Huang, R., Zhang, Y., Bozzetti, C., Ho, K., Cao, J., Han, Y., Daellenbach, K. R., Slowik, J. G., Platt, S.

607 M., Canonaco, F., Zotter, P., Wolf, R., Pieber, S. M., Bruns, E. A., Crippa, M., Ciarelli, G.,  
608 Piazzalunga, A., Schwikowski, M., Abbaszade, G., Schnelle-Kreis, J., Zimmermann, R., An, Z.,  
609 Szidat, S., Baltensperger, U., Haddad, I. E., and Prévôt, A. S. H.: High secondary aerosol  
610 contribution to particulate pollution during haze events in China, *Nature*, 514(7521), 218-222,  
611 <http://dio.org/10.1038/nature13774>, 2014.

612 Hwa, M., and Yu, T.: Development of real-world driving cycles and estimation of emission factors  
613 for in-use light-duty gasoline vehicles in urban areas, *Environ Monit Assess*, 186, 3985-3994,  
614 <http://dio.org/10.1007/s10661-014-3673-1>, 2014.

615 Jacobson, M. Z.: Strong radiative heating due to the mixing state of black carbon in atmospheric aerosols,  
616 *Nature*, 409(6821), 695-697, <http://dio.org/10.1038/35055518>, 2001.

617 Jang, M. S., Czoschke, N. M., Lee, S., and Kamens, R. M.: Heterogeneous atmospheric aerosol  
618 production by acid-catalyzed particle-phase reactions, *Science*, 298(5594), 814-817,  
619 <http://dio.org/10.1126/science.1075798>, 2002.

620 Jang, M., Czoschke, N. M., and Northcross, A. L.: Atmospheric organic aerosol production by  
621 heterogeneous acid-catalyzed reactions, *Chemphyschem*, 5(11), 1647-1661,  
622 <http://dio.org/10.1002/cphc.200301077>, 2004.

623 Jathar, S. H., Gordon, T. D., Hennigan, C. J., Pye, H. O. T., Pouliot, G., Adams, P. J., Donahue, N. M.,  
624 and Robinson, A. L.: Unspeciated organic emissions from combustion sources and their influence  
625 on the secondary organic aerosol budget in the United States, *P. Natl. Acad. Sci. USA*, 111(29),  
626 10473-10478, <http://dio.org/10.1073/pnas.1323740111>, 2014.

627 Kanakidou, M., Seinfeld, J. H., Pandis, S. N., Barnes, I., Dentener, F. J., Facchini, M. C., Van Dingenen,  
628 R., Ervens, B., Nenes, A., Nielsen, C. J., Swietlicki, E., Putaud, J. P., Balkanski, Y., Fuzzi, S., Horth,  
629 J., Moortgat, G. K., Winterhalter, R., Myhre, C., Tsigaridis, K., Vignati, E., Stephanou, E. G., and  
630 Wilson, J.: Organic aerosol and global climate modelling: A review, *Atmos. Chem. Phys.*, 5, 1053-  
631 1123, <http://dio.org/10.5194/acp-5-1053-2005>, 2005.

632 Khalek, I. A., Bougher, T., and Jetter, J. J.: Particle Emissions from a 2009 gasoline direct injection  
633 engine using different commercially available fuels, *SAE Int. J. Fuels Lubr.*, 3(2), 623- 637,  
634 <http://dio.org/10.4271/2010-01-2117>, 2010.

635 Kuwata, M., Liu, Y., McKinney, K., and Martin, S.T.: Physical state and acidity of inorganic sulfate  
636 can regulate the production of secondary organic material from isoprene photooxidation  
637 products, *Phys Chem Chem Phys: PCCP*, 17, 5670-5678, <http://dio.org/10.1039/C4CP04942J>,  
638 2015.

639 Lack, D.A., Langridge, J.M., Bahreini, R., Cappa, C.D., Middlebrook, A.M., and Schwarz, J.P.:  
640 Brown carbon and internal mixing in biomass burning particles, *P Natl Acad Sci USA*, 109,  
641 <http://dio.org/14802-14807>, 10.1073/pnas.1206575109, 2012.

642 Lambe, A.T., Ahern, A.T., Wright, J.P., Croasdale, D.R., Davidovits, P., and Onasch, T.B.:  
643 Oxidative aging and cloud condensation nuclei activation of laboratory combustion soot, *J*  
644 *Aerosol Sci.*, 79, 31-39, <http://dio.org/10.1016/j.jaerosci.2014.10.001>, 2015.

645 Lang-Yona, N., Abo-Riziq, A., Erlick, C., Segre, E., Trainic, M., and Rudich, Y.: Interaction of  
646 internally mixed aerosols with light, *Phys Chem Chem Phys*, 12, 21-31,  
647 <http://dio.org/10.1039/B913176K>, 2010.

648 Laskin, A., Laskin, J., and Nizkorodov, S.A.: Chemistry of Atmospheric Brown Carbon, *Chem Rev*,  
649 115, 4335-4382, <http://dio.org/10.1021/cr5006167>, 2015.

650 Li, W., and Shao, L.: Transmission electron microscopy study of aerosol particles from the brown hazes

651 in northern china, *J. Geophys. Res.-Atmos.*, <http://dio.org/D09302>, 2009.

652 Liati, A., Schreiber, D., Dasilva, Y. A. R., and Eggenschwiler, P. D.: Ultrafine particle emissions from  
653 modern gasoline and diesel vehicles: An electron microscopic perspective, *Environ. Pollut.*, 239,  
654 661-669, <http://dio.org/10.1016/j.envpol.2018.04.081>, 2018.

655 Liu, L., Kong, S., Zhang, Y., Wang, Y., Xu, L., Yan, Q., Lingaswamy, A. P., Shi, Z., Lv, S., Niu, H.,  
656 Shao, L., Hu, M., Zhang, D., Chen, J., Zhang, X., and Li, W.: Morphology, composition, and mixing  
657 state of primary particles from combustion sources - crop residue, wood, and solid waste, *Sci. Rep.-*  
658 *UK*, <http://dio.org/10.1038/s41598-017-05357-2>, 2017.

659 Loh, N.D., Hampton, C.Y., Martin, A.V., Starodub, D., Sierra, R.G., Barty, A., Aquila, A., Schulz,  
660 J., Lomb, L., Steinbrener, J., Shoeman, R.L., Kassemeyer, S., Bostedt, C., Bozek, J., Epp, S.W.,  
661 Erk, B., Hartmann, R., Rolles, D., Rudenko, A., Rudek, B., Foucar, L., Kimmel, N.,  
662 Weidenspointner, G., Hauser, G., Holl, P., Pedersoli, E., Liang, M., Hunter, M.M., Gumprecht,  
663 L., Coppola, N., Wunderer, C., Graafsma, H., Maia, F.R.N.C., Ekeberg, T., Hantke, M.,  
664 Fleckenstein, H., Hirsemann, H., Nass, K., White, T.A., Tobias, H.J., Farquar, G.R., Benner,  
665 W.H., Hau-Riege, S.P., Reich, C., Hartmann, A., Soltau, H., Marchesini, S., Bajt, S.,  
666 Barthelmess, M., Bucksbaum, P., Hodgson, K.O., Strueder, L., Ullrich, J., Frank, M.,  
667 Schlichting, I., Chapman, H.N., and Bogan, M.J.: Fractal morphology, imaging and mass  
668 spectrometry of single aerosol particles in flight, *Nature*, 486, 513-517,  
669 <http://dio.org/10.1038/nature11222>, 2012.

670 Lu, K.D., Hofzumahaus, A., Holland, F., Bohn, B., Brauers, T., Fuchs, H., Hu, M., Häßeler, R., Kita,  
671 K., Kondo, Y., Li, X., Lou, S.R., Oebel, A., Shao, M., Zeng, L.M., Wahner, A., Zhu, T., Zhang,  
672 Y.H., and Rohrer, F.: Missing OH source in a suburban environment near Beijing: observed  
673 and modelled OH and HO<sub>2</sub> concentrations in summer 2006, *Atmos Chem Phys*, 13, 1057-1080,  
674 <http://dio.org/10.5194/acp-13-1057-2013>, 2013.

675 Luo, Y., Zhu, L., Fang, J., Zhuang, Z., Guan, C., Xia, C., Xie, X., and Huang, Z.: Size distribution,  
676 chemical composition and oxidation reactivity of particulate matter from gasoline direct injection  
677 (GDI) engine fueled with ethanol-gasoline fuel, *Appl. Therm. Eng.*, 89, 647-655,  
678 <http://dio.org/10.1016/j.applthermaleng.2015.06.060>, 2015.

679 Ma, Q., Wu, Y., Zhang, D., Wang, X., Xia, Y., Liu, X., Tian, P., Han, Z., Xia, X., Wang, Y., and  
680 Zhang, R.: Roles of regional transport and heterogeneous reactions in the PM<sub>2.5</sub> increase during  
681 winter haze episodes in Beijing, *Sci Total Environ*, 599, 246-253,  
682 <http://dio.org/10.1016/j.scitotenv.2017.04.193>, 2017.

683 Maricq, M. M., Szente, J., Loos, M., and Vogt, R.: Motor vehicle PM emissions measurement at LEV  
684 III levels, *SAE Int. J. Engines*, 4(1), 597- 609, <http://dio.org/10.4271/2011-01-0623>, 2011.

685 Mauldin, R. L. I., Berndt, T., Sipilä, M., Paasonen, P., Petaja, T., Kim, S., Kurten, T., Stratmann, F.,  
686 Kerminen, V., and Kulmala, M.: A new atmospherically relevant oxidant of sulphur dioxide, *Nature*,  
687 488(7410), 193-196, <http://dio.org/10.1038/nature11278>, 2012.

688 National Bureau of Statistics of China, 2018. China Statistical Yearbook 2018, part sixteen:  
689 Transportation, post and telecommunications and software industry. Available on line at:  
690 <http://www.stats.gov.cn/tjsj/ndsj/2018/indexch.htm>, 2018.

691 Niu, H., Cheng, W., Hu, W., and Pian, W.: Characteristics of individual particles in a severe short-period  
692 haze episode induced by biomass burning in Beijing, *Atmos. Pollut. Res.*, 7(6), 1072-1081,  
693 <http://dio.org/10.1016/j.apr.2016.05.011>, 2016.

694 Niu, H., Hu, W., Zhang, D., Wu, Z., and Guo, S.: Variations of fine particle physiochemical



695 properties during a heavy haze episode in the winter of Beijing, *Sci Total Environ*, 571, 103-  
696 109, <http://dio.org/10.1016/j.scitotenv.2016.07.147>, 2016.

697 Niu, H., Shao, L., and Zhang, D.: Aged status of soot particles during the passage of a weak cyclone in  
698 Beijing, *Atmos. Environ.*, 45(16), 2699-2703, <http://dio.org/10.1016/j.atmosenv.2011.02.056>, 2011.

699 Okada, K., Qin, Y., and Kai, K.: Elemental composition and mixing properties of atmospheric mineral  
700 particles collected in Hohhot, China, *Atmos. Res.*, 73(1-2), 45-67,  
701 <http://dio.org/10.1016/j.atmosres.2004.08.001>, 2005.

702 Peng, J., Hu, M., Guo, S., Du, Z., Shang, D., Zheng, J., Zheng, J., Zeng, L., Shao, M., Wu, Y., Collins,  
703 D., and Zhang, R.: Ageing and hygroscopicity variation of black carbon particles in Beijing  
704 measured by a quasi-atmospheric aerosol evolution study (QUALITY) chamber, *Atmos. Chem.*  
705 *Phys.*, 17(17), 10333-10348, <http://dio.org/10.5194/acp-17-10333-2017>, 2017.

706 Peng, J.F., Hu, M., Wang, Z.B., Huang, X.F., Kumar, P., Wu, Z.J., Guo, S., Yue, D.L., Shang, D.J.,  
707 Zheng, Z., and He, L.Y.: Submicron aerosols at thirteen diversified sites in China: size distribution,  
708 new particle formation and corresponding contribution to cloud condensation nuclei production,  
709 *Atmos Chem Phys*, 14, 10249-10265, 10.5194/acp-14-10249-2014, 2014.

710 Petzold, A., Marsh, R., Johnson, M., Miller, M., Sevcenco, Y., Delhaye, D., Ibrahim, A., Williams, P.,  
711 Bauer, H., Crayford, A., Bachalo, W. D., and Raper, D.: Evaluation of methods for measuring  
712 particulate matter emissions from gas turbines, *Environ. Sci. Technol.*, 45(8), 3562-3568, 2011.

713 Rönkkö, T., Löhde, T., Heikkilä, J., Pirjola, L., Bauschke, U., Arnold, F., Schlager, H., Rothe, D., Yli-  
714 Ojanperä, J., and Keskinen, J.: Effects of gaseous sulphuric acid on diesel exhaust nanoparticle  
715 formation and characteristics, *Environ. Sci. Technol.*, 47(20), 11882-11889,  
716 <http://dio.org/10.1021/es402354y>, 2013.

717 Scott, C. E., Rap, A., Spracklen, D. V., Forster, P. M., Carslaw, K. S., Mann, G. W., Pringle, K. J.,  
718 Kivekas, N., Kulmala, M., Lihavainen, H., and Tunved, P.: The direct and indirect radiative effects  
719 of biogenic secondary organic aerosol, *Atmos. Chem. Phys.*, 14(1), 447-470,  
720 <http://dio.org/10.5194/acp-14-447-2014>, 2014.

721 Shao, L., Hu, Y., Fan, J., Wang, J., Wang, J., and Ma, J.: Physicochemical characteristics of aerosol  
722 particles in the Tibetan Plateau: Insights from TEM-EDX analysis, *J. Nanosci. Nanotechnol.*, 17(9),  
723 6899-6908, <http://dio.org/10.1166/jnn.2017.14472>, 2017.

724 Shao, L., Hu, Y., Shen, R., Schärer, K., Wang, J., Wang, J., Schnelle-Kreis, J., Zimmermann, R., Bédouin,  
725 K., and Suppan, P.: Seasonal variation of particle-induced oxidative potential of airborne particulate  
726 matter in Beijing, *Sci. Total Environ.*, 579, 1152-1160,  
727 <http://dio.org/10.1016/j.scitotenv.2016.11.094>, 2017.

728 Song, C., Na, K., Warren, B., Malloy, Q., and Cocker, D.R.: Secondary Organic Aerosol Formation from  
729 m-Xylene in the Absence of NO<sub>x</sub>, *Environ Sci Technol*, 41, 7409-7416,  
730 <http://dio.org/10.1021/es070429r>, 2007.

731 Song, M., Zhang, C., Wu, H., Mu, Y., Ma, Z., Zhang, Y., Liu, J., and Li, X.: The influence of OH  
732 concentration on SOA formation from isoprene photooxidation, *Sci Total Environ*, 650, 951-957,  
733 <http://dio.org/10.1016/j.scitotenv.2018.09.084>, 2019.

734 Shi, Z., Vu, T., Kotthaus, S., Harrison, R. M., Grimmond, S., Yue, S., Zhu, T., Lee, J., Han, Y., Demuzere,  
735 M., Dunmore, R. E., Ren, L., Liu, D., Wang, Y., Wild, O., Allan, J., Acton, W. J., Barlow, J., Barratt,  
736 B., Beddows, D., Bloss, W. J., Calzolari, G., Carruthers, D., Carslaw, D. C., Chan, Q., Chatzidiakou,  
737 L., Chen, Y., Crilly, L., Coe, H., Dai, T., Doherty, R., Duan, F., Fu, P., Ge, B., Ge, M., Guan, D.,  
738 Hamilton, J. F., He, K., Heal, M., Heard, D., Hewitt, C. N., Holloway, M., Hu, M., Ji, D., Jiang, X.,

739 Jones, R., Kalberer, M., Kelly, F. J., Kramer, L., Langford, B., Lin, C., Lewis, A. C., Li, J., Li, W.,  
740 Liu, H., Liu, J., Loh, M., Lu, K., Lucarelli, F., Mann, G., McFiggans, G., Miller, M. R., Mills, G.,  
741 Monk, P., Nemitz, E., O'Connor, F., Ouyang, B., Palmer, P. I., Percival, C., Popoola, O., Reeves,  
742 C., Rickard, A. R., Shao, L., Shi, G., Spracklen, D., Stevenson, D., Sun, Y., Sun, Z., Tao, S., Tong,  
743 S., Wang, Q., Wang, W., Wang, X., Wang, X., Wang, Z., Wei, L., Whalley, L., Wu, X., Wu, Z.,  
744 Xie, P., Yang, F., Zhang, Q., Zhang, Y., Zhang, Y., and Zheng, M.: Introduction to the special issue  
745 "In-depth study of air pollution sources and processes within Beijing and its surrounding region  
746 (APHH-Beijing)", *Atmos. Chem. Phys.*, 19(11), 7519-7546, [http://dio.org/10.5194/acp-19-7519-](http://dio.org/10.5194/acp-19-7519-2019)  
747 2019, 2019.

748 Suarez-Bertoa, R., Zardini, A. A., Platt, S. M., Hellebust, S., Pieber, S. M., El Haddad, I., Temime-  
749 Roussel, B., Baltensperger, U., Marchand, N., Prévôt, A. S. H., and Astorga, C.: Primary emissions  
750 and secondary organic aerosol formation from the exhaust of a flex-fuel (ethanol) vehicle, *Atmos.*  
751 *Environ.*, 117, 200-211, <http://dio.org/10.1016/j.atmosenv.2015.07.006>, 2015.

752 Szybist, J. P., Youngquist, A. D., Barone, T. L., Storey, J. M., and Moore, W. R.: Ethanol blends and  
753 engine operating strategy effects on light-duty spark-ignition engine particle emissions, *Energ. Fuel.*,  
754 25(11), 4977-4985, <http://dio.org/10.1021/ef201127y>, 2011.

755 Wang, W., Shao, L., Li, J., Chang, L., Zhang, D., Zhang, C., and Jiang, J.: Characteristics of individual  
756 particles emitted from an experimental burning chamber with coal from the lung cancer area of  
757 Xuanwei, China, *Aerosol Air Qual. Res.*, 19(2), 355-363, <http://dio.org/10.4209/aaqr.2018.05.0187>,  
758 2019.

759 Xing, J., Shao, L., Zhang, W., Peng, J., Wang, W., Hou, C., Shuai, S., Hu, M., and Zhang, D.:  
760 Morphology and composition of particles emitted from a port fuel injection gasoline vehicle under  
761 real-world driving test cycles, *J. Environ. Sci-China*, 76, 339-348,  
762 <http://dio.org/10.1016/j.jes.2018.05.026>, 2019.

763 Xing, J., Shao, L., Zheng, R., Peng, J., Wang, W., Guo, Q., Wang, Y., Qin, Y., Shuai, S., and Hu, M.:  
764 Individual particles emitted from gasoline engines: Impact of engine types, engine loads and fuel  
765 components, *J. Clean. Prod.*, 149, 461-471, <http://dio.org/10.1016/j.jclepro.2017.02.056>, 2017.

766 Yu, L., Wang, G., Zhang, R., Zhang, L., Song, Y., Wu, B., Li, X., An, K., and Chu, J.: Characterization  
767 and source apportionment of PM<sub>2.5</sub> in an urban environment in Beijing, *Aerosol Air Qual. Res.*,  
768 13(2), 574-583, 2013.

769 Zhang, H., Cheng, S., Li, J., Yao, S., and Wang, X.: Investigating the aerosol mass and chemical  
770 components characteristics and feedback effects on the meteorological factors in the  
771 Beijing-Tianjin-Hebei region, China, *Environ. Pollut.*, 244, 495-502,  
772 <http://dio.org/10.1016/j.envpol.2018.10.087>, 2019.

773 Zhang, M., Li, Z., Xu, M., Yue, J., Cai, Z., Yung, K.K.L., and Li, R.: Pollution characteristics,  
774 source apportionment and health risks assessment of fine particulate matter during a  
775 typical winter and summer time period in urban Taiyuan, China, *Hum Ecol Risk Assess.*,  
776 <http://dio.org/10.1080/10807039.2019.1684184>, 2019.

777 Zhang, Y., Yuan, Q., Huang, D., Kong, S., Zhang, J., Wang, X., Lu, C., Shi, Z., Zhang, X., Sun, Y.,  
778 Wang, Z., Shao, L., Zhu, J., and Li, W.: Direct observations of fine primary particles from residential  
779 coal burning: Insights into their morphology, composition, and hygroscopicity, *J. Geophys. Res.-*  
780 *Atmos.*, 123(22), 12,964-12,979, <http://dio.org/10.1029/2018JD028988>, 2018.

781 Zhu, J., Penner, J. E., Lin, G., Zhou, C., Xu, L., and Zhuang, B.: Mechanism of SOA formation  
782 determines magnitude of radiative effects, *P. Natl. Acad. Sci. USA*, 114(48), 12685-12690,

783 <http://dio.org/10.1073/pnas.1712273114>, 2017.  
784 Zimmerman, N., Wang, J. M., Jeong, C., Ramos, M., Hilker, N., Healy, R. M., Sabaliauskas, K., Wallace,  
785 J. S., and Evans, G. J.: Field measurements of gasoline direct injection emission factors: Spatial and  
786 seasonal variability, *Environ. Sci. Technol.*, 50(4), 2035-2043,  
787 <http://dio.org/10.1021/acs.est.5b04444>, 2016.

788

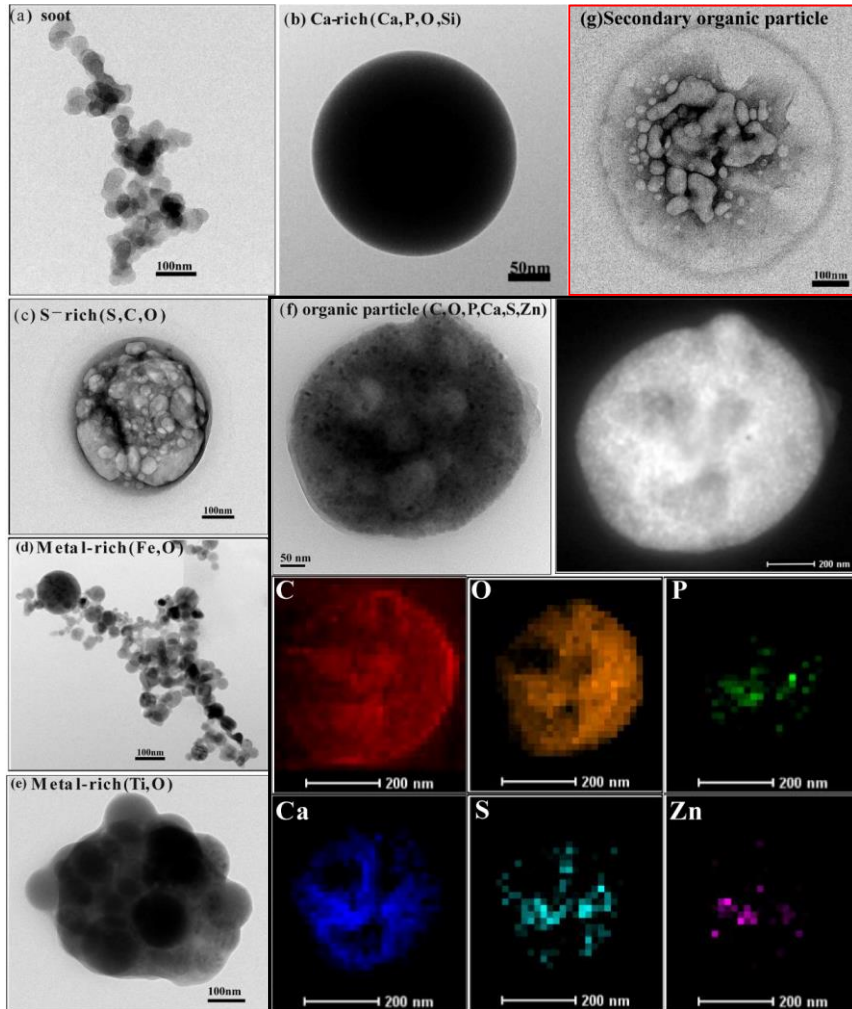
789 **List of tables:**790 Table 1 Comparison of chemical components between various sources including fossil  
791 fuels, biomass burning and urban waste burning

Study	Source	Particle of type and relative percentages	Chemical composition of organic particles
This study	GDI-engine vehicles	Organic particles (OM) (32%), Soot (32%), Ca-rich particles (26%), S-rich (5%) and metal-containing particles (4%)	OM with Ca and weak P, S, and Zn
Xing et al. (2019)	PFI-engine vehicles	OM (44%), soot (23%), Ca-rich particles (20%), S-rich (6%) and metal-containing particles (6%).	OM with Ca and weak P, S, and Zn.
Liati et al. (2018)	GDI, PFI and diesel vehicles	Soot, OM (called ash-bearing soot particles) and ash particles.	OM with Ca, S, P, Fe and minor Zn.
Liu et al. (2017)	Crop residue combustion	OM (27%), OM-K (43%), OM-soot-K (27%), soot-OM (3%).	OM particles with K content.
Liu et al. (2017)	Wood combustion	OM (16%), soot (18%), OM-K (22%), OM-soot-K (15%), soot-OM (29%).	OM particles with K content.
Wang et al. (2019)	Coal burning	OM (38%), soot (40%), S-rich particles (2%), and mineral particles (18%).	OM mainly consisted of C, O and Si.
Zhang et al. (2018)	Residential coal burning	OM (51%), OM-S (24%), soot-OM (23%), S-rich (1%), metal-rich particles (1%), mineral particles (1%).	OM contained C, O, and Si with minor amounts of S and Cl.

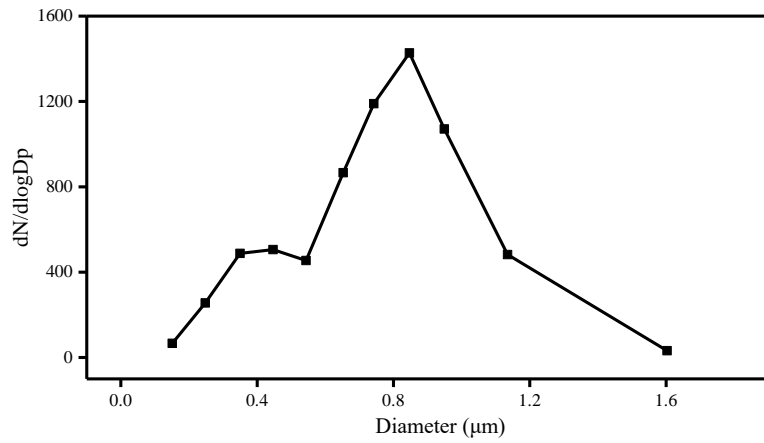
792

793

794 **List of figures:**



795  
 796 Figure 1. TEM images of the individual primary particles emitted from the GDI-engine  
 797 gasoline vehicle and the secondary organic particle in the chamber after exposure to  
 798 ambient sunlight for 3.5 hours. (a) soot particle; (b) Ca-rich particle; (c) S-rich particles;  
 799 (d) Metal-rich particles (Fe); (e) Metal-rich particles (Ti); (f) bright-field-TEM and  
 800 dark-field-TEM image of organic particles, and others are the mapping of the C, O, P,  
 801 Ca, S, and Zn in the organic particle; (g) secondary organic particle in chamber.  
 802



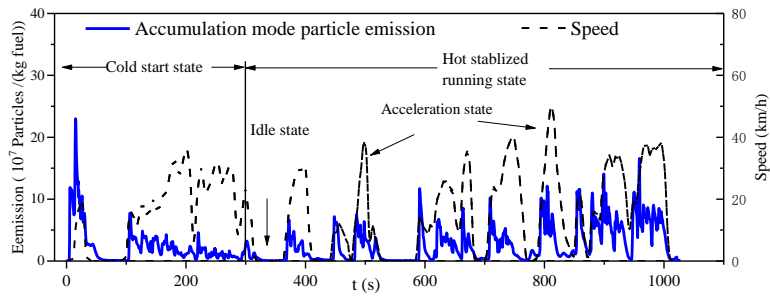
803

804 Figure 2. Size distribution of analyzed particles emitted from the GDI-engine gasoline  
805 vehicles by the TEM images. In total, 2880 particles were analyzed from the GDI-  
806 engine vehicles. Particles smaller than 0.25 µm should have been underestimated  
807 because of the collection efficiency of the impactor.

808

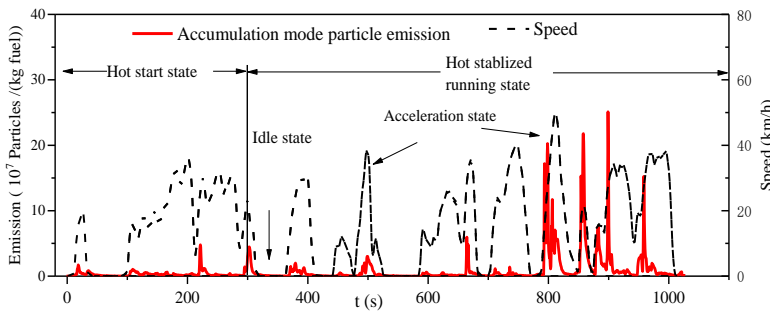
809

810 (a)



811

812 (b)



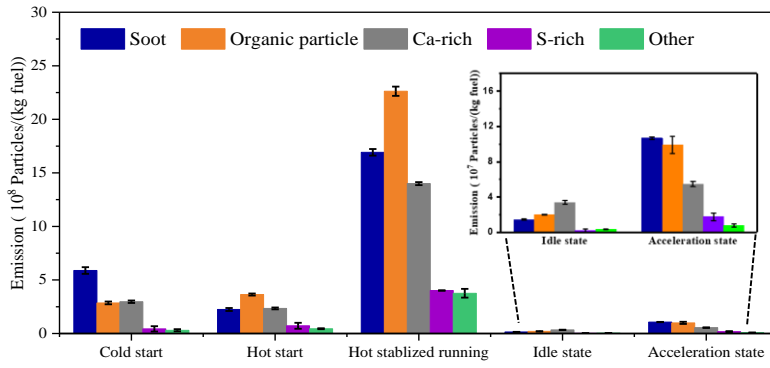
813

814 Figure 3. Particles in accumulation mode from the GDI vehicle during cold start (a) and  
815 hot start (b) driving cycle. The vehicle speed is also shown for reference. Before the  
816 test with cold start, the temperatures of the engine coolant and oil could not differ by  
817 more than 2 °C during the soak temperature. The hot start test was conducted within 5  
818 mins after the cold start test. The number concentration of particles during the tests was  
819 monitored by DMS 500.

820

821

822

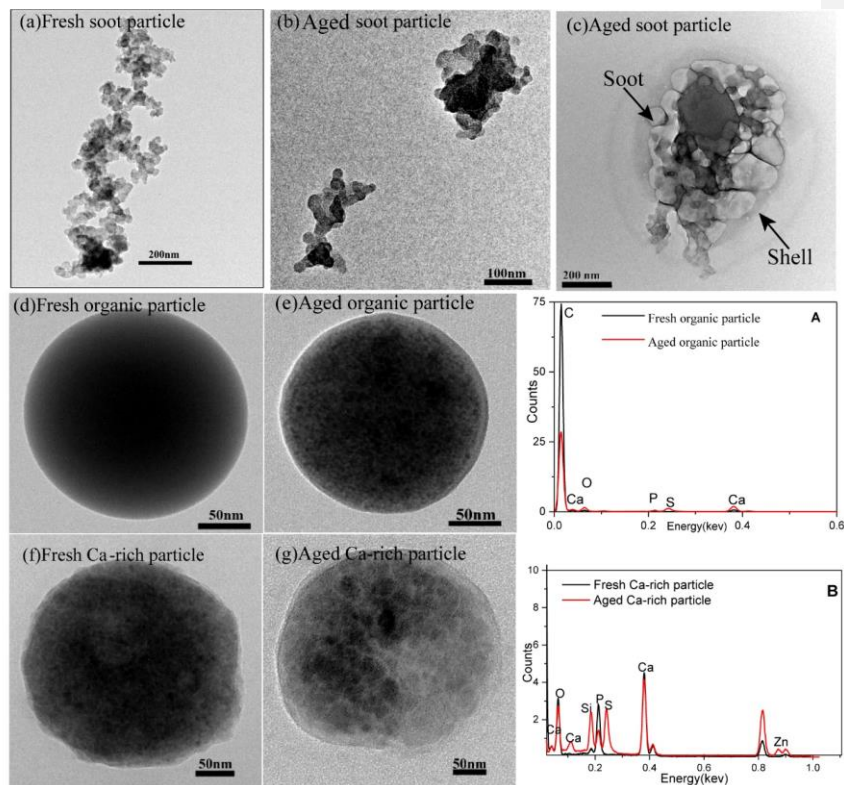


823

824 Figure 4. The number of different type particles in the emissions from the GDI vehicle  
825 under the different running states by the burning of per unit of fuel, including cold start,  
826 hot start, hot stabilization, idle, and acceleration states. Data presented as  
827 mean  $\pm$  standard deviation, N = 3.

828





829

830 Figure 5. TEM images of particles in the chamber after exposure to ambient sunlight  
 831 for 3.5 hours. (a) Fresh soot particles; (b) Aged soot particles; (c) Aged soot particle (d)  
 832 Fresh organic particle (e) Aged organic particle (f) Fresh Ca-rich particle (g) Aged Ca-  
 833 rich particle (A) EDX spectrum for a fresh organic particle and an aged organic particle.  
 834 (B) EDX spectrum for a fresh organic particle and an aged Ca-rich particle.